

Original article

Morphometric measurements of posterior cranial fossa and craniovertebral junction in Chiari I malformation with and without Syringohydromyelia

Pawitra Imemkamon, Supada Prakkamakul, Ketsuda Jakchairoongruang*

Department of Radiology, Faculty of Medicine, Chulalongkorn University, King Chulalongkorn Memorial Hospital, Thai Red Cross Society, Bangkok, Thailand

Background: Syringohydromyelia occurs about 30.0% – 85.0% in patients with Chiari I malformation (CMI). The syrinx formation is supposed to be a result of disturbed cerebrospinal fluid flow dynamics, which is associated with the degree of mechanical blockage that may be related to posterior cranial fossa (PCF) and craniovertebral junction anatomy.

Objective: Our study aimed to determine the morphometric difference in PCF and craniocervical junction between the CMI patients with and without syringohydromyelia.

Methods: Thirty CMI patients (16 with syringohydromyelia; 14 without syringohydromyelia) and 16 healthy subjects were also recruited. PCF and craniocervical junction measurements of 5 distances and 5 angles were performed. Comparison of these measurements was employed among the three groups.

Results: The clivus length and Klaus index in the CMI patients were shorter than in the controls ($P = 0.002$ and $P < 0.001$). The twining line was shorter in the CMI patients without syringohydromyelia when compared to the controls ($P = 0.046$). The Boogard's and Nasion-basion-Opisthion (NBO) angles were larger, and the clivus gradient angle was smaller in the CMI patients with syringohydromyelia than the controls ($P = 0.009$, $P = 0.014$, and $P = 0.009$). Degree of tonsillar descent, the distances and the angles were not significantly different between the CMI patients with and without syringohydromyelia.

Conclusion: Our study showed no difference in PCF and craniocervical junction morphometry between CMI patients with and without syringohydromyelia. The results support that CMI patients has underdeveloped PCF and more clivus horizontal orientation than the healthy subjects. Large population study with evaluation of mechanical and functional factors may help understanding and predicting the risk of syrinx formation among CMI individual.

Keywords: Chiari I, syringohydromyelia, measurement, craniocervical junction, posterior cranial fossa.

Chiari I malformation (CMI) is the most common variant of the Chiari malformation, which originates from the abnormality of embryonic hindbrain development that can be associated with syringohydromyelia. CMI is characterized by cerebellar tonsils that are abnormally shaped and downwardly displaced beyond the level of foramen magnum > 5 millimeters.⁽¹⁾

Symptoms and neurological dysfunction of patients with CMI are secondary to hindbrain compression and the presence of syringohydromyelia, which includes severe headache with neck pain, occipital headache, loss of pain and temperature sensation, loss of muscle strength, dizziness, or balance problem. However, many patients with CMI are asymptomatic.

Syringohydromyelia is identified in 30.0% – 85.0% of patients with CMI.⁽²⁾ Disturbed cerebrospinal fluid (CSF) flow dynamics in CSF flow studies, the association between the degree of mechanical blockage, and the formation of syrinx are believed to be a result of posterior cranial fossa (PCF) and craniocervical abnormalities.⁽³⁻⁵⁾

*Correspondence to: Ketsuda Jakchairoongruang, Faculty of Medicine, Chulalongkorn University, King Chulalongkorn Memorial Hospital, The Thai Red Cross Society, Bangkok 10330, Thailand.

E-mail: ketsuda.ja@chula.ac.th

Received: April 27, 2021

Revised: July 29, 2021

Accepted: September 14, 2021

To our knowledge, craniocervical junction abnormalities, such as basilar invagination, platybasia, small posterior cranial fossa, abnormal concavity of the clivus, and retroverted odontoid process, were found in some patients with CMI.^(2, 6, 7) Previous studies suggested that these abnormalities may be associated with the presence of syringohydromyelia in CMI when compared to those without.⁽⁶⁾ Several previous studies have focused on the morphometric difference between patients with CMI and normal populations^(8 - 14), but only few studies provide information among CMI with syrinx group and without syrinx group.⁽¹⁵⁾ The purposes of our study were: 1) to determine whether there is the morphometric difference in posterior cranial fossa and craniovertebral junction between the CMI patients with and without syringohydromyelia; and 2) to identify other craniocervical junction abnormalities in the CMI patients.

Materials and methods

Patients

In this institutional review board approved study, we retrospectively reviewed the imaging on patients diagnosed with Chiari I malformation between June 2002 - December 2018 at King Chulalongkorn Memorial Hospital. We searched for cases from the

hospital electronic radiologic/medical records, including records with the terms “Chiari I malformation”, “tonsillar ectopia”, and “low-lying tonsils”. The inclusion criteria were: 1) patients over 18 years old diagnosed with Chiari I malformation (tonsillar descent beyond foramen magnum > 5 mm) with and without syringomyelia; 2) patients who underwent standard MR imaging of the brain and whole spine in KCMH. The exclusion criteria were: 1) history of skull trauma or decompressive, cranial/spinal surgery; 2) any tonsillar herniation secondary to space-occupying lesion; 3) presence of other spinal abnormality that would cause syringohydromyelia; and 4) poor image quality.

Initially, 41 Chiari I malformation patients were identified. Eleven patients were excluded due to inadequate imaging (n = 6), history of skull surgery (n = 2) and tonsillar descent less than 5 mm (n = 3). A total of 30 CMI patients were consequently classified into two groups: 1) CMI with syringohydromyelia (n = 16); and, 2) CMI without syringohydromyelia (n = 14). (Figure 1)

We recruited 16 patients whose MRI brain and whole spine showed normal appearance of posterior cranial fossa (PCF) and cerebellar tonsils as the control group.

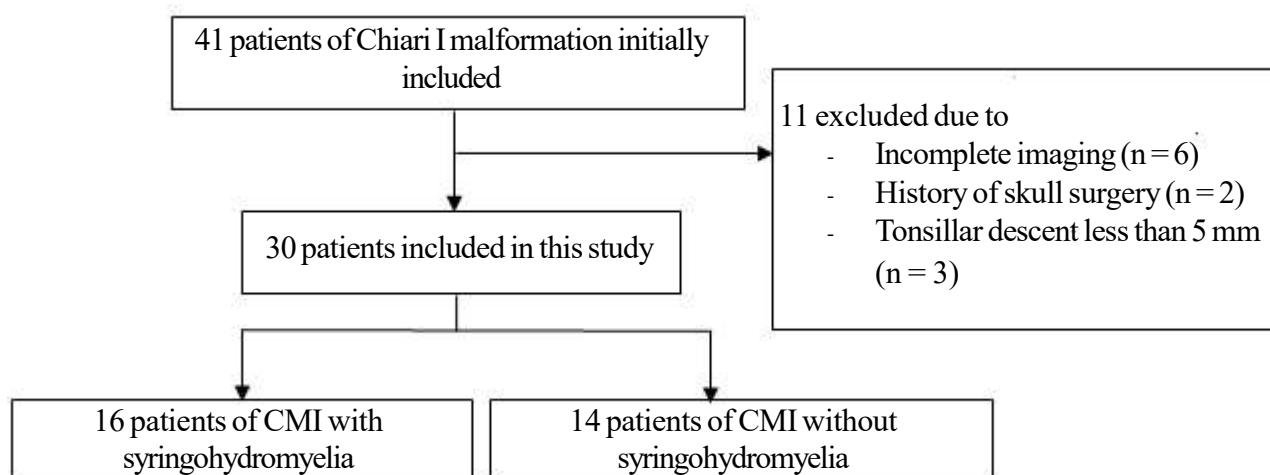


Figure 1. Flowchart of patient selection.

MR images selection and evaluation

MR images of subjects were reviewed. The MRI images were performed either on 1.5 or 3.0 Tesla scanners. Scanners were sourced from the following vendors: General Electric (Discovery 750 w), Philips (Ingenia), and Siemens (Skyra, Aera). Routine imaging protocol of MRI brain studies included T1-weighted images in sagittal plane (TR/TE 410 - 520/10 - 20 ms; flip angle 70 - 90; field of view 220 - 250 mm) and T2-weighted images in axial plane (TR/TE 3300 - 6000/90 - 130 ms; flip angle 90 - 150; field of view 220 - 250 mm) spin-echo techniques with 5 mm section thickness and 1 mm intersection gaps. Sagittal 3D T1-weighted images gradient echo were obtained in a few patients with 1.6 mm section thickness and 0.8 mm intersection gaps. Sagittal MRI spine studies included T2-weighted images were obtained (TR/TE 2500 - 4040/94 - 120 ms; flip angle

90 - 150; field of view 180 - 290 mm) using spin-echo techniques with 3 - 5 mm section thickness and 0.3 - 1.0 mm intersection gaps.

Image assessment was performed on the Picture Archiving and Communication System (PACS). Morphometric measurement on Sagittal T1-weighted spin-echo images or Sagittal 3D T1-weighted gradient echo images (if available) were independently assessed by two neuroradiologists, KJ and SP (7-year experience), who were blinded to the diagnosis. Mid sagittal T1-weighted images were used for measurements of the posterior cranial fossa and craniocervical junction. The measurement of the length of syringohydromyelia was performed on spinal mid sagittal T2-weighted images by one neuroradiologist (KJ). The mean of all measurements from both readers were used for the analyses (Figure 2 - 4).

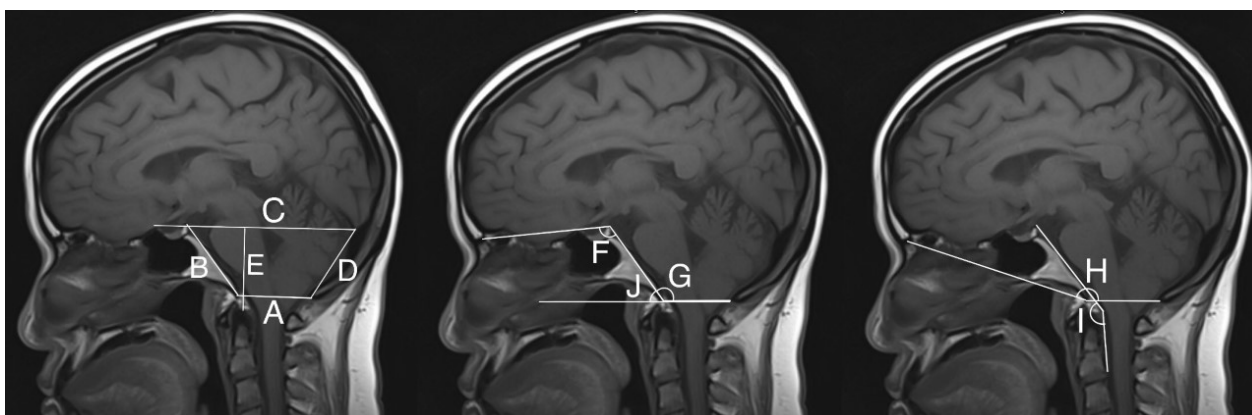


Figure 2. Morphometric measurements on mid sagittal T1-weighted image; A. McRae line, B. Clivus length, C. Twining line, D. IOP-O line, E. Klaus index, F. Basal angle, G. Boogard's angle, H. NBO angle, I. Clivus canal angle J. Clivus angle.

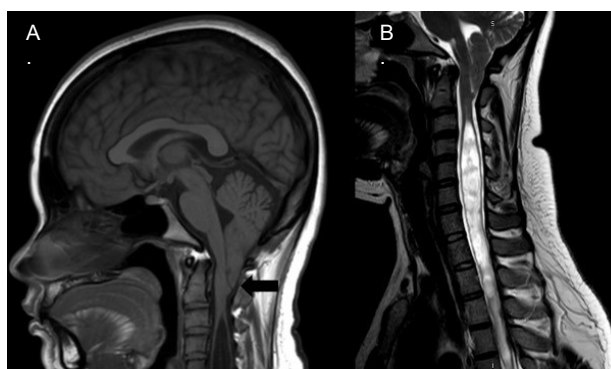


Figure 3. A 34-year-old female, Chiari I malformation with syringomyelia; (A) Sagittal T1-weighted MR image of the brain shows peg-like tonsillar descent (arrow) and partially seen syrinx formation in upper cervical cord; (B) Sagittal T2-weighted MR image of the cervical spine demonstrates long segment of syringohydromyelia extending from C2 level down to thoracic level.

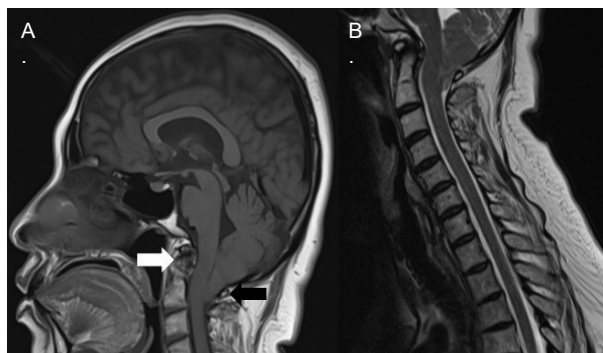


Figure 4. A 55-year-old female, Chiari I malformation without syringomyelia: **(A)** Sagittal T1-weighted MR image of the brain shows peg-like tonsillar descent (black arrow). Retroverted odontoid process is present (white arrow); **(B)** Sagittal T2-weighted MR image of the cervical spine demonstrates normal spinal cord without demonstrable syringohydromyelia.

The measurements applied to evaluate posterior cranial fossa and craniocervical junction (5 distances and 5 angles) included: the distances: 1) McRae line (distance from basion to opisthion); 2) Clivus length (distance between dorsum selle to basion); 3) Twining line (distance between tuberculum sellae to internal occipital protuberance); 4) Klaus index (distance from tip of odontoid to twining line, representing posterior fossa height); and, 5) IOP-P line (distance between internal occipital protuberance to opisthion); and the angles: 1) Basal angle (angle of line extending across anterior cranial fossa to dorsum selle and the line along posterior margin of clivus); 2) Boogard's angle (angle between the clivus and McRae line); 3) Nasion-basion-opisthion (NBO) angle (angle formed by nasion-basion-opisthion); and, 4) Clivus canal angle (angle of the line along clivus and the line of posterior to odontoid process); and, 5) Clivus gradient (angle formed by line extended from McRae line and clivus) (Figure 5)

Degree of tonsillar descent, the length of syrinx, and other craniocervical osseous abnormalities were recorded.

Statistical analysis

All statistical analysis was performed with SPSS 22.0 software. The measurement data were compared between CMI with syringohydromyelia, CMI without syringohydromyelia, and the control group. Continuous variables are presented as mean \pm standard deviation (SD). Categorical variables are presented as count and percentage. Comparisons of continuous variables were performed using one-way analysis of variance (One-way ANOVA) and student *t* - test. Comparison of categorical variables was performed using the chi-square (χ^2) test. Pearson's correlation coefficient was used to find the correlation between the length of syrinx and any measurements. *P* - value < 0.05 was considered statistically significant.

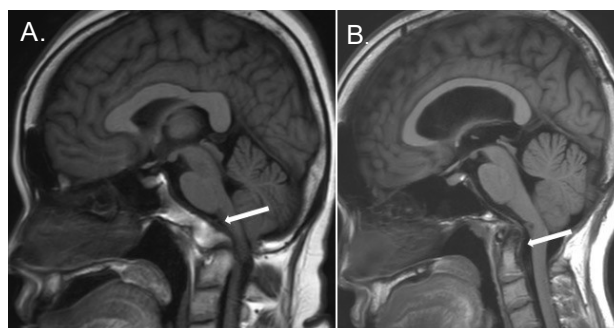


Figure 5. Associated craniocervical junction abnormalities in CMI: **(A)** Sagittal T1-weighted MR image in a 46-year-old female patient; CMI with syringohydromyelia shows abnormal fusion of clivus and C1 (arrow) with short and retroverted odontoid process. Compression of cervicomedullary junction is depicted; **(B)** Sagittal T1-weighted MR brain image in a 54-year-old female patient diagnosed CMI without syringohydromyelia demonstrates retroflexion of odontoid process indenting cervicomedullary junction (arrow).

Results

Sixteen of thirty CMI patients (53.0%) had syringohydromyelia. In CMI group with syringohydromyelia, there were 6 males and 10 females, and the mean age was 41.4 ± 11.7 years (range 25 - 58 years). One male and thirteen females were in CMI groups without syringohydromyelia with the mean age of 50.5 ± 14.8 years (range 20 - 65 years). In control group, there were 7 males and 9 females, and the mean age was 46.1 ± 13.2 years (range 24 - 64 years). Demographic data are shown in Table 1. There was no significant difference of age and gender among these three groups.

The degree of tonsillar descent was 10.5 ± 5.9 mm in CMI group with syringohydromyelia and 11.3 ± 6.5 mm in CMI without syringohydromyelia, which showed no statistically significant difference between these two groups ($P = 0.547$). All patients in CMI with syringohydromyelia group had syrinx in the

cervical level. Ten of sixteen patients had the syrinx extended down to thoracic level and one patient into L1 level (Table 2).

Posterior cranial fossa and craniocervical junction measurements on MRI of three groups (CMI with syringohydromyelia, CMI without syringohydromyelia and control groups) were shown in Table 3 and Table 4. The clivus length and Klaus index were significantly shorter in CMI group (both with and without syringohydromyelia) when compared to control group ($P = 0.002$ and < 0.001 , respectively). Distance of twining line was significantly shorter in CMI without syringohydromyelia when compared to control group ($P = 0.046$). However, there was no significant difference in these measurements between CMI with and without syringohydromyelia groups. The distance of McRae line and IOP-O line showed no significant difference among the three groups.

Table 1. Demographic data.

Mean \pm SD	CMI with syrinx (n = 16) (%)	CMI without syrinx (n = 14) (%)	Control group (n = 16) (%)	P - value
Age (years)	41.4 (± 11.7)	50.50 (± 14.9)	46.1 (± 13.2)	0.186
Gender				
Male	6 (37.5)	1 (7.2)	7 (43.8)	
Female	10 (62.5)	13 (92.8)	9 (56.3)	0.072
Degree of tonsillar descent (mm)	10.5 (± 5.9)	11.3 (± 6.5)	-	0.547
Length of syrinx (Vertebral segments)	8.4 (± 6.6)			

Table 2. Location of the syringohydromyelia.

Spine level	Total (n = 16)	
Cervical	16	Isolated C level = 6
Thoracic	10	C-T level = 9
Lumbar	1	C-T-L level = 1

Table 3. Comparison of measurement of the distance between three groups.

Distance Mean \pm SD	CMI with syrinx (n = 16)	CMI without syrinx (n = 14)	Control group (n = 16)	P - value
McRae line (cm)	3.3 ± 0.4	3.3 ± 0.2	3.5 ± 0.2	0.061
Clivus length (cm)	4.2 ± 0.5	4.1 ± 0.4	4.7 ± 0.4	0.002 ^{a,b}
Twining line (cm)	9.1 ± 0.6	8.8 ± 0.4	9.3 ± 0.7	0.046 ^b
IOP-O line (cm)	4.0 ± 0.5	3.9 ± 0.4	4.3 ± 0.4	0.061
Klaus index (cm)	3.7 ± 0.5	3.8 ± 0.6	4.6 ± 0.4	< 0.001 ^{a,b}

a = statistically significant difference between CMI with syrinx and control group

b = statistically significant difference between CMI without syrinx and control group

Table 4. Comparison of measurement of the angles between three groups.

Angle Mean \pm SD	CMI with syrx (n = 16)	CMI without syrx (n = 14)	Control group (n = 16)	P - value
Basal angle	116.9 \pm 7.7	15.2 \pm 4.2*	114.6 \pm 5.1	0.545
Boogard's angle	31.3 \pm 12.2	125.7 \pm 12.7	119.0 \pm 6.5	0.009 ^a
NBO angle	169.7 \pm 10.1	163.2 \pm 13.2*	158.0 \pm 8.7	0.014 ^a
Clivus canal angle	144.2 \pm 16.6	147.1 \pm 12.0	154.3 \pm 8.2	0.081
Clivus gradient angle	48.7 \pm 12.2	54.3 \pm 12.7	61.0 \pm 6.5	0.009 ^a

a = statistically significant different between CMI with syrx and control group

* Only 9 patients with these measurements were done due to some with unable to be measured from the available imaging.

As for the angle measurements, Boogard's angle and NBO angle were larger in CMI with syringohydromyelia group than control group ($P = 0.009$ and 0.014 , respectively). The clivus gradient angle was significantly smaller in CMI with syringohydromyelia group than control group ($P = 0.009$). There was no difference in these angles between CMI patients with and without syringohydromyelia. Basal angle and Clivus canal angle did not differ among these three groups.

In addition, we found no statistically significant correlation between length of syrx and any measurements. Associated findings were: 1) hydrocephalus (n = 2; one CMI with syringohydromyelia and one without); 2) abnormality at craniocervical junction, including fusion C0/1 with anteflexion of odontoid process (n = 1, CMI with syringohydromyelia group), retroposition or retroflexion of odontoid process (n = 2, CMI without syringohydromyelia). Most of the patients (14 of 16 patients in CMI with syringohydromyelia and 13 of 14 patients in CMI without syringohydromyelia) did not have osseous abnormality at the craniocervical junction.

Interobserver agreement

We found good to excellent interobserver agreement between two readers for all measurements. Interclass correlation coefficients were 0.85 (95% confidence interval [CI]: 0.74 - 0.92) for McRae line, 0.92 (95% CI: 0.84 - 0.95) for Clivus length, 0.93 (95% CI: 0.87 - 0.96) for Twining line, 0.89 (95% CI: 0.81 - 0.94) for IOP-O line, 0.98 (95% CI: 0.96 - 0.99) for Klaus index, 0.74 (95% CI: 0.51 - 0.86) for Basal angle, 0.96 (95% CI: 0.94 - 0.98) for Boogard angle, 0.97 (95% CI: 0.94 - 0.98) for NBO angle, 0.86 (95% CI: 0.81 - 0.94) for Clivus canal angle and 0.96 (95% CI: 0.94 - 0.98) for Clivus gradient.

Discussion

Chiari malformations are a group of disorder defined by the abnormality of embryonic hindbrain development in relation to the foramen magnum and the skull base and were first described in 1891.^(5, 16) The resulting compaction and crowding at the craniocervical junction in CMI are believed to cause disruption of normal CSF flow as shown in previous CSF flow studies that may result in syringohydromyelia.

Yan H, *et al.* found that CMI with syrx group tend to have more degree of tonsillar descent when compared to non-syrinx group.⁽¹⁵⁾ Our study failed to demonstrate the difference in degree of tonsillar descent between these two groups. Strover LJ, *et al.* reported that syrx degree was lower in mild herniation⁽¹⁷⁾, nevertheless, there was no significant correlation in terms of degree of tonsillar herniation and the length of syrx in our study.

Our study showed only three CMI patients with craniocervical osseous abnormality: one with atlanto-occipital fusion and reflexion of the odontoid process and two with retroflexion of the odontoid process. Previous studies significantly observed craniocervical junction abnormalities such as basilar invagination, platybasia, abnormal concavity of clivus and retroverted odontoid process in CMI particularly in young children.^(6, 18) Gad KA, *et al.* studied these osseous abnormalities and syrx formation, which revealed significant association between syrx formation and craniocervical abnormalities.⁽⁶⁾ The reason we found only few patients with these osseous abnormalities was probably due to our study focusing on adult population.

Many previous studies focused on the dimension and morphological assessment of the posterior cranial fossa in patients with CMI compared to normal

population.^(8 - 15, 19) Most of them showed different morphologic measurements between these two groups. Alkoc OA, *et al.* demonstrated significantly wider Boogard angle, shorter Klaus index, clivus length and IOP-O distance in CMI than normal population.⁽⁸⁾ Houston JR, *et al.* also illustrated significantly longer McRae line, shorter clivus length, wider basal angle, wider Boogard angle and smaller clivus canal angle in CMI than normal population.⁽⁹⁾ Karagoz F, *et al.* showed tendency of platybasia on angle measurements in the Chiari group including wider basal angle, Boogard angle, NBO angle and shorter anteroposterior length of PCF (Twining line).⁽¹¹⁾ Several other previous studies also showed these differences in similar way^(14, 15, 20, 21), which were believed to be due to underdevelopment of the occipital bone and posterior cranial fossa in CMI patients. Nevertheless, they did not assess the morphometric difference of posterior cranial fossa in forming syringohydromyelia in CMI.

Our study disclosed that clivus length, Twining line (reflecting anteroposterior diameter of posterior cranial fossa) and Klaus index (reflecting height of the posterior cranial fossa) were significantly lower in CMI patients when compared to healthy subjects. The distance of McRae line and IOP-O line were also lower than the control group, but the study failed to show statistically significant. These findings were similar to several previous literatures and support the pathogenesis theory of underdevelopment of the PCF in Chiari malformation.^(8 - 15, 19) No significant difference of PCF morphometry was observed in our study when we compared between syringohydromyelia group and non-syringohydromyelia group.

For angular measurements of craniocervical junction, previous studies suggested that wide basal and Boogard angles (providing evidence of horizontal angulation of the clivus), and narrow Clivus canal angle (reflecting basilar invagination), were morphological characteristic for CMI.^(6, 9, 11, 20) Our study found Boogard angle and NBO angle to be statistically significant wider in CMI with syringohydromyelia group than the control group. Clivus gradient angle was also narrower in CMI with syringohydromyelia than the control group. These results were similar to previous studies and can postulate that CMI is related to more horizontal angulation of clivus. The clivus canal angle in CMI were slightly narrower in our study, however, there was no statistically significant difference. Unlike in previous studies, we failed to show basal angle difference among these three

groups. This could result from our study having only few patients with osseous craniocervical junction abnormality in CMI patients with syringohydromyelia. In a previous CSF flow study, Brunck AC, *et al.* showed abnormal maximum velocities at the craniocervical junction which was significantly decreased in CMI, especially in CMI with syrinx group.⁽⁴⁾ Pinna G, *et al.* also showed different CSF flow dynamics in those with syrinx and without syrinx, which is believed to have been caused by the junctional obstruction in syrinx group.⁽²²⁾ However, our study revealed no statistically significant difference in PCF morphometric distances and angles between CMI with syringohydromyelia group and non-syringohydromyelia group. These findings might raise a possibility that the PCF morphometry might not be the only key factor for development of syringohydromyelia. There might be other contributing factors associated with syrinx formation.

In the CMI with syringohydromyelia group, all our patients had the syrinx in the cervical cord. Ten out of sixteen had syrinx extended to the thoracic level and rarely extended to lumbar level (1/16). None of patients had isolated syrinx in the thoracic or the lumbar level. These results differed from Kennedy BC, *et al.* study that isolated thoracic syrinx without involvement of the cervical cord was found in 9.1% in CMI children with syrinx in their study.⁽²³⁾ This study recommends an entire spinal cord imaging in initial evaluation for CMI children to prevent missed diagnosis and to aid surgical decision.

Our study had some limitations, however. First, small number of patients were included. In addition, Basal and NBO angles could not be performed in some patients due to the lack of image coverage in anatomical landmarks. Second, we found difficulty in identifying the exact anatomical points for the measurements in some patients due to their anatomical variations, particularly on 2D T1-weighted images, which may affect the accuracy of the measurements. Third, the presence of syrinx in the upper cervical level included in the MR imaging of the brain might cause bias. Finally, the development of the syrinx is believed to be a dynamic process. Our retrospectively at one point of time might not accurately represent the true existence of the syrinx. Future study with larger number of patients both children and adult, using 3D T1-weighted images with whole spine imaging, and follow-up might give additional information about the posterior cranial fossa morphometry and might predict syrinx formation in CMI.

Our study supports the hypothesis that patients with Chiari I malformation has underdeveloped or small posterior cranial fossa and more horizontal angulation of clivus than the normal population. Among Chiari I malformation with and without syringohydromyelia, our results did not show morphometric difference of the posterior cranial fossa and craniocervical junction between those. Future study with larger study population with evaluation of mechanical and functional factors may help understanding and predicting the risk of syrinx formation among CMI individual.

Conflict of interest

The authors have no conflict of interest to disclose.

References

1. Caldarelli M, Di Rocco C. Diagnosis of Chiari I malformation and related syringomyelia: radiological and neurophysiological studies. *Childs Nerv Syst* 2004;20:332-5.
2. Milhorat TH, Chou MW, Trinidad EM, Kula RW, Mandell M, Wolpert C, et al. Chiari I malformation redefined: clinical and radiographic findings for 364 symptomatic patients. *Neurosurgery* 1999;44:1005-17.
3. Fernández AA, Guerrero AI, Martínez MI, Vázquez MA, Fernández JB, Chesa i Octavio E, et al. Malformations of the craniocervical junction (Chiari type I and syringomyelia: classification, diagnosis and treatment). *BMC Musculoskeletal Disord* 2009; 10 Suppl 1:S1.
4. Bunck AC, Kroeger JR, Juettner A, Brentrup A, Fiedler B, Crelmer GR, et al. Magnetic resonance 4D flow analysis of cerebrospinal fluid dynamics in Chiari I malformation with and without syringomyelia. *Eur Radiol* 2012;22:1860-70.
5. Oldfield EH. Pathogenesis of Chiari I - pathophysiology of syringomyelia: implications for therapy: a summary of 3 decades of clinical research. *Neurosurgery* 2017; 64(CN_suppl_1):66-77.
6. Gad KA, Yousem DM. Syringohydromyelia in patients with Chiari I malformation: a retrospective analysis. *AJNR Am J Neuroradiol* 2017;38:1833-8.
7. Moore HE, Moore KR. Magnetic resonance imaging features of complex Chiari malformation variant of Chiari I malformation. *Pediatr Radiol* 2014;44:1403-11.
8. Alkoc OA, Songur A, Eser O, Toktas M, Gonul Y, Esi E, et al. Stereological and morphometric analysis of MRI Chiari malformation type-1. *J Korean Neurosurg Soc* 2015;58:454-61.
9. Houston JR, Eppelheimer MS, Pahlavian SH, Biswas D, Urbizu A, Martin BA, et al. A morphometric assessment of type I Chiari malformation above the McRae line: A retrospective case-control study in 302 adult female subjects. *J Neuroradiol* 2018;45:23-31.
10. Furtado SV, Reddy K, Hegde AS. Posterior fossa morphometry in symptomatic pediatric and adult Chiari I malformation. *J Clin Neurosci* 2009;16:1449-54.
11. Karagoz F, Izgi N, Kapijicijoglu Sencer S. Morphometric measurements of the cranium in patients with Chiari type I malformation and comparison with the normal population. *Acta Neurochir (Wien)* 2002;144:165-71.
12. Furtado SV, Thakre DJ, Venkatesh PK, Reddy K, Hegde AS. Morphometric analysis of foramen magnum dimensions and intracranial volume in pediatric Chiari I malformation. *Acta Neurochir* 2010;152:221-7.
13. Urbizu A, Poca MA, Vidal X, Rovira A, Sahuquillo J, Macaya A. MRI-based morphometric analysis of posterior cranial fossa in the diagnosis of Chiari malformation type I. *J Neuroimaging* 2014;24:250-6.
14. Dufton JA, Habeeb SY, Heran MK, Mikulis DJ, Islam O. Posterior fossa measurements in patients with and without Chiari I malformation. *Can J Neurol Sci* 2011;38:452-5.
15. Yan H, Han X, Jin M, Liu Z, Xie D, Sha S, et al. Morphometric features of posterior cranial fossa are different between Chiari I malformation with and without syringomyelia. *Eur Spine J* 2016;25:2202-9.
16. Schijman E. History, anatomic forms, and pathogenesis of Chiari I malformations. *Childs Nerv Syst* 2004;20: 323-8.
17. Stovner LJ, Bergan U, Nilsen G, Sjaastad O. Posterior cranial fossa dimensions in the Chiari I malformation: relation to pathogenesis and clinical presentation. *Neuroradiology* 1993;35:113-8.
18. Elster AD, Chen MY. Chiari I malformations: clinical and radiologic reappraisal. *Radiology* 1992;183:347-53.
19. Nishikawa M, Sakamoto H, Hakuba A, Nakanishi N, Inoue Y. Pathogenesis of Chiari malformation: a morphometric study of the posterior cranial fossa. *J Neurosurgery* 1997;86:40-7.
20. Schady W, Metcalfe RA, Butler P. The incidence of craniocervical bony anomalies in the adult Chiari malformation. *J Neurol Sci* 1987;82:193-203.
21. Dagtekin A, Avci E, Kara E, Uzmansel D, Dagtekin O, Koseoglu A, et al. Posterior cranial fossa morphometry in symptomatic adult Chiari I malformation patients: comparative clinical and anatomical study. *Clin Neurol Neurosurg* 2011;113:399-403.

22. Pinna G, Alessandrini F, Alfieri A, Rossi M, Bricolo A. Cerebrospinal fluid flow dynamics study in Chiari I malformation: implications for syrinx formation. *Neurosurg Focus* 2000;8:E3.
23. Kennedy BC, Kelly KM, Anderson RC, Feldstein NA. Isolated thoracic syrinx in children with Chiari I malformation. *Childs Nerv Syst* 2016;32:531-4.